Ocean Engineering 38 (2011) 186–196

Contents lists available at ScienceDirect

Ocean Engineering

journal homepage: www.elsevier.com/locate/oceaneng

Neuro-fuzzy based approach for wave transmission prediction of horizontally interlaced multilayer moored floating pipe breakwater

S.G. Patil [a,*], S. Mandal [b], A.V. Hegde [c], Srinivasan Alavandar [d]

[a] Department of Built and Natural Environment, Caledonian College of Engineering, P.O. Box: 2322, CPO Seeb, PC 111, Sultanate of Oman
[b] Ocean Engineering Division, National Institute of Oceanography, Goa 403 004, India
[c] Department of Applied Mechanics and Hydraulics, National Institute of Technology Karnataka, Surathkal, Srinivasnagar, Mangalore 575025, India
[d] Department of Electronics and Computer Engineering, Caledonian College of Engineering, P.O. Box: 2322, CPO Seeb, PC 111, Sultanate of Oman

ARTICLE INFO

Article history:
Received 6 April 2010
Accepted 17 October 2010
Editor-in-Chief: A.I. Incecik
Available online 4 November 2010

Keywords:
Neuro-fuzzy
ANFIS
Floating breakwater
HIMMFPB
Wave transmission

ABSTRACT

The ocean wave system in nature is very complicated and physical model studies on floating breakwaters are expensive and time consuming. Till now, there has not been available a simple mathematical model to predict the wave transmission through floating breakwaters by considering all the boundary conditions. This is due to complexity and vagueness associated with many of the governing variables and their effects on the performance of breakwater. In the present paper, Adaptive Neuro-Fuzzy Inference System (ANFIS), an implementation of a representative fuzzy inference system using a back-propagation neural network-like structure, with limited mathematical representation of the system, is developed. An ANFIS is trained on the data set obtained from experimental wave transmission of horizontally interlaced multilayer moored floating pipe breakwater using regular wave flume at Marine Structure Laboratory, National Institute of Technology Karnataka, Surathkal, India. Computer simulations conducted on this data shows the effectiveness of the approach in terms of statistical measures, such as correlation coefficient, root-mean-square error and scatter index. Influence of input parameters is assessed using the principal component analysis. Also results of ANFIS models are compared with that of artificial neural network models.

1. Introduction

There is a great volume of published work dealing with floating breakwaters (Bishop, 1982; Harms, 1979; Harris and Webber, 1968; Homma et al., 1964; Kennedy and Marsalek, 1968; Leach, McDougal and Solitt, 1985), but it is noticed that there is a lack of a simple mathematical model to predict breakwater performance characteristics, such as the transmission coefficient. A number of studies has been carried out considering a floating breakwater in basic form with some assumptions common in hydrodynamics, which shows less improvement.

In the last two decades, floating breakwaters (Mani, 1991; McCartney, 1985; Murali and Mani, 1997; Sannasiraj et al., 1998; Sundar et al., 2003) have generated a great interest in the field of coastal engineering, as they are less expensive compared to conventional type breakwaters. In addition, they have several desirable characteristics, such as, comparatively small capital cost, adoption to varying harbour shapes and sizes, short construction time and freedom from silting and scouring. Floating breakwaters could also be utilized to meet location changes, extent of protection required or seasonal demand. They can be used as a temporary protection for offshore activities in hostile environment during construction, drilling works, salvage operation, etc. For an effective design of floating pipe breakwater, it is necessary to study the hydrodynamic performance characteristics of this structure. Hence, a study on wave transmission of the floating pipe breakwater would provide a proper configuration to the structure.

In recent years, the research interest in Artificial Neural Networks (ANN) has increased and many efforts have been made on applications of neural networks to various coastal engineering problems. An ANN in coastal/ocean engineering is commonly used by the researchers to predict ocean wave parameters like wave height, wave period, impact wave force, etc. (Deo et al., 2001; Deo and Jagdale, 2003; Gunaydin, 2008; Londhe and Deo, 2003). Apart from this, it has provided promising results in the prediction of tidal levels (Chang and Lin, 2006), damages to coastal structures (Mandal et al., 2007), depth of eroded caves in a seawall (Lee et al., 2009), seabed liquefaction (Jeng et al., 2004), storm surges (Tseng et al., 2007), etc. The most significant features of neural networks are the extreme flexibility, due to learning ability and the capability of nonlinear function approximations. This fact leads us to expect neural networks to be an excellent tool for solving the motion characteristics of the floating pipe breakwater, while overcoming

* Corresponding author.
E-mail addresses: sanras5@gmail.com (S.G. Patil), smandal@nio.org (S. Mandal), arkalvittal@gmail.com (A.V. Hegde), seenu.phd@gmail.com (S. Alavandar).

0029-8018/$ - see front matter © 2010 Elsevier Ltd. All rights reserved.
doi:10.1016/j.oceaneng.2010.10.009

complexity and non-linearity associated with wave-structure interaction.

Fuzzy inference systems are the most popular constituent of the soft computing area, since they are able to represent the human expertise in the form of IF antecedent THEN consequent statements. In this domain, the system behavior is modeled through the use of linguistic descriptions. Although the earliest work by Zadeh (1965) on fuzzy systems has not been paid the attention which it deserved in early 1960s, since then the methodology has become a well-developed framework. The typical architecture of fuzzy inference systems (FIS) is introduced by Wang (1994, 1997), Takagi and Sugeno (1985) and Jang et al. (1997). A fuzzy system having generalized bell membership function, product inference rule and weighted average defuzzifier has become the standard method in most applications. Takagi and Sugeno (1985) change the defuzzification procedure, where dynamic systems are introduced as defuzzification subsystems.

Many researchers have developed a hybrid model by combining the neural network with fuzzy logic for solving coastal engineering problems (Bakhtyar et al., 2008a; Bateni and Jeng, 2007; Chang and Chien, 2006; Kazeminezhad et al., 2005). Ozger and Zekai (2006) have adopted dynamic fuzzy approach to identify the effect of wind speed on wave characteristics variations in an ocean wave generating system. Bakhtyar et al. (2008b) have concluded that the ANFIS model is more flexible than the FIS model, with more options for incorporating the fuzzy nature of the real world system. Sylaios et al. (2009) have used Takagi-Sugeno (1985) rule based fuzzy inference system for forecasting wave parameters based on the wind speed and direction, and the lagged wave characteristics. They used subtractive clustering method to identify the initial and final antecedent fuzzy membership functions. Yagci et al. (2005) have used fuzzy logic method in breakwater damage ratio estimation. Erdik (2009) has applied the fuzzy logic approach in design of conventional rubble mound structures. However, it is observed that there are hardly any applications of soft computing tools on the wave transmission of floating breakwater.

In the present paper, the performance of an ANFIS for predicting wave transmission coefficient of horizontally interlaced multilayer moored floating pipe breakwater (HIMMFPB) is investigated. Influence of input parameters is assessed using the principal component analysis (PCA). Results of ANFIS models are compared with that of artificial neural network models (Mandal et al., 2009). The paper is organized as follows—Section 1 starts with the literature associated with floating breakwaters and applications of soft computing techniques in coastal engineering. Section 2 details wave transmission of floating breakwater and experimental HIMMFPB. Section 3 describes the structure of an ANFIS used. Data and application of an ANFIS are described in Section 4. Results and discussions are described in Section 5. Conclusions and acknowledgments are presented in Sections 6 and 7, respectively.

2. Wave transmission of floating breakwater

Floating breakwaters are based on the concept of either reflecting the wave energy or dissipating wave energy by an induced turbulent motion. In recent times, many types of floating breakwater models have been tested and some have been constructed and their prototype performances have been assessed. Floating breakwaters can be subdivided into five general types: Box, Pontoon, Mat, Tethered float and Pipe. The prime factor in the construction of the floating breakwaters is to make the width of the breakwater (in the direction of wave propagation) greater than one half the wavelengths and preferably as wide as the incident wavelength; else, the breakwater rides over the top of the wave without attenuating it. Also to be effective, the floating breakwater must be moored in place with both leeward and windward ties; otherwise it would sag off and ride over the incident wave. Pontoon and Box types of floating breakwaters belong to the first category, in which the wave attenuation is achieved by reflecting the wave energy. Mat and Tethered belong to the other category, in which wave energy dissipation is mainly due to drag from the resultant float in motion. Pipe breakwaters mainly dissipate the wave energy, and partly reflect and transmit the waves.

2.1. About experimental HIMMFPB model

The development of floating breakwaters by various investigations has been influenced by certain important features; large masses, large moment of inertia, and the combinations of two. Most of the literature indicates that the parameter "relative width" influences greatly the wave attenuation characteristics of the breakwater.

The details of the HIMMFPB are shown in Fig. 1 (Deepak, 2006; Hegde et al., 2007; Jagadisha, 2007; Kamat, 2010). The breakwater comprises of the rigid poly vinyl chloride (PVC) pipes. These pipes are placed parallel to each other with certain spacing between them in each layer and the adjacent layers are oriented at right angles to each other, so as to form an interlacing. Longitudinal pipes are placed along the direction of propagation of waves and transverse pipes are placed and tied perpendicular to longitudinal pipes. The length of the longitudinal pipes defines the width of the breakwater. It is felt that with proper number of layers, spacing of pipes and relative breakwater width, it is possible to achieve a considerable and effective attenuation of waves. Fig. 1 shows a pictorial representation of the HIMMFPB model in plan and section. The wave-specific parameters and structure-specific parameters considered in the experiments are shown in Table 1. The experimental study carried out by Kamat (2010) shows hydrodynamic characteristics of horizontally interlaced three and five layer floating breakwater systems, in which the wave transmission is less for five layer systems. These experimental data are divided into two sets, one for training and other for testing the ANFIS models (Table 2).

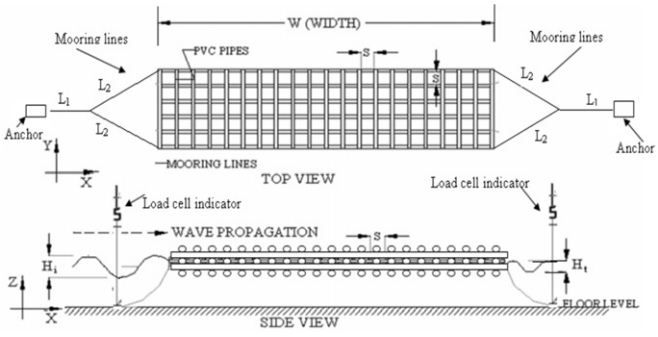

Fig. 1. HIMMFPB model setup.

Table 1
Range of wave-specific and structure-specific parameters used in HIMMFPB.

Wave-specific parameters	**Experimental range**
Incident wave height, H_i (mm)	30, 60, 90, 120, 150, 180
Wave period, T (s)	1.2, 1.4, 1.6, 1.8, 2.0, 2.2
Depth of water, d (mm)	400, 450, 500
Structure-specific parameters	**Experimental range**
Diameter of pipes, D (mm)	32
Ratio of spacing to diameter of pipes, S/D	2, 3, 4 and 5
Relative breakwater width, W/L	0.4–2.65
Number of layers, n	5

Table 2
Data used for training and testing the network models.

S/D ratio	Data for training	Data for testing	Total data
2	609	203	812
3	576	233	809
4	366	143	509
5	581	234	815
Combined total	2132	813	2945

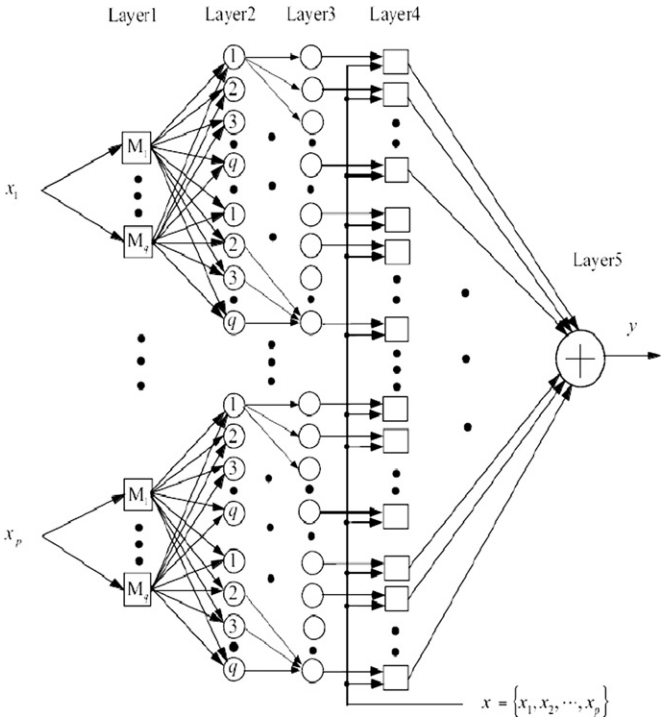

Fig. 2. ANFIS structure.

3. ANFIS architecture

Inspired by the idea of basing the fuzzy logic inference procedure on a feed forward network structure, Jang (1993) proposed a fuzzy neural network model—the Adaptive Neural Fuzzy Inference System or semantically equivalent, Adaptive Network-based Fuzzy Inference System (ANFIS), whose architecture is shown in Fig. 2. Jang (1993) reported that the ANFIS architecture can be employed to model nonlinear functions, identify nonlinear components on-line in a control system, and predict a chaotic time series. It is a hybrid neuro-fuzzy technique that brings learning capabilities of neural networks to fuzzy inference systems. The learning algorithm tunes the membership functions of a Sugeno-type Fuzzy Inference System, using the training set of input–output data. A detailed coverage of an ANFIS can be found in Jang (1993), Jang et al. (1997) and Srinivasan and Nigam (2008). The ANFIS, from the topology point of view, is an implementation of a representative fuzzy inference system using a back-propagation neural network-like structure. It consists of five layers. The role of each layer is briefly presented as follows: let O_i^l denote the output of the node i in the layer l and x_i is the i^{th} input of the ANFIS, $i=1, 2, \ldots, p$. In layer 1, there is a node function M associated with every node

$$O_i^l = M_i(x_i) \tag{1}$$

The role of the node functions $M_1, M_2, \ldots, M_q$ here is same as the membership functions $\mu(x)$ used in the regular fuzzy systems, and q is the number of nodes for each input. Generalized bell membership function is the typical choice. The adjustable parameters that determine the positions and shapes of these node functions are referred to as the premise parameters. The output of every node in layer 2 is the product of all the incoming signals

$$O_i^2 = M_l(x_l) \quad AND \quad M_j(x_j) \tag{2}$$

Each node output represents the firing strength of the reasoning rule. In layer 3, each of these firing strengths of the rule is compared with the sum of all the firing strengths. Therefore, the normalized firing strengths are compared in this layer as

$$O_i^3 = \frac{O_i^2}{\sum_i O_i^2} \tag{3}$$

Layer 4 implements the Sugeno-type inference system, i.e. a linear combination of the input variables of an ANFIS $x_1, x_2, \ldots, x_p$ plus a constant term $c_1, c_2, \ldots, c_p$, from the output of each *IF–THEN* rule. The output of the node is a weighted sum of these intermediate outputs

$$O_i^4 = O_i^3 \sum_{j=1}^{p} (P_j x_j + c_j) \tag{4}$$

where parameters $P_1, P_2, \ldots, P_p$ and $c_1, c_2, \ldots, c_p$, in this layer are referred to as the consequent parameters. The node in layer 5 produces the sum of its inputs, i.e. the defuzzification process of the fuzzy system (using weighted average method) and is obtained as

$$O_i^5 = \sum_i O_i^4 \tag{5}$$

The present paper considers the ANFIS structure with first order Sugeno model containing 27 fuzzy rules and 3 generalized bell membership functions for ANFIS1, ANFIS2, ANFIS3 and ANFIS4 models, whereas for ANFIS5 model 81 fuzzy rules and 3 generalized bell membership functions are used. At the fuzzification level, all ANFIS models use product inference rule and hybrid learning algorithm that combines least square method with gradient descent method to adjust the parameter of membership functions, whereas weighted average is used as defuzzifier.

4. Data and fuzzy logic approach

Data used to train and test all ANFIS models are obtained from physical model experiments on HIMMFPB using the regular wave flume at the Marine Structure Laboratory, National Institute of Technology Karnataka, Surathkal, India (Deepak, 2006; Hegde et al., 2007; Jagadisha, 2007). The input parameters that influence the wave transmission (K_t) of floating pipe breakwater, such as spacing of pipes relative to pipe diameter (S/D), breakwater width relative to wave length (W/L), incident wave relative to water depth (H_i/d) and incident wave relative to wave length (H_i/L) are considered. Based on the above input parameters, six ANFIS models are constructed to predict the transmission coefficient of HIMMFPB as shown in Table 3.

W/L, H_i/d, H_i/L and K_t are used as a training data to train ANFIS1, ANFIS2, ANFIS3 and ANFIS4 network having an S/D ratio as 2, 3, 4 and 5, respectively. Experimental analysis shows that K_t is better with an increase in S/D ratio, in this regard to study over a range of an S/D on K_t, an input parameter, S/D is added to form an ANFIS5 model. An ANFIS6 model is the same as ANFIS5 model without H_i/L parameter. The number of data used for training and testing for all ANFIS models is shown in Table 3. The codes are written in MATLAB 7 Release 14.

From the experimental data, surface graphs are obtained to show the variation of K_t (Z-axis) with respect to various two parameters (X- and Y-axis) at a time (Fig. 3). The same set of data is used to train the ANFIS models. In all these figures, K_t is same and depicts the non-linearity and complexity associated in mapping input and output parameters of HIMMFPB.

The flowchart of an ANFIS procedure used in the present paper is shown in Fig. 4. In the first step, initialization of the fuzzy system is done using *genfis1* command, which specifies the structure and initial parameters of the fuzzy inference system (FIS) with training data matrix, number of membership functions and membership function type associated with each input. In the above, the number

Table 3
ANFIS models with input parameters.

Model	*S/D* ratio	Input parameters
ANFIS1	2	W/L, H_i/d, H_i/L
ANFIS2	3	W/L, H_i/d, H_i/L
ANFIS3	4	W/L, H_i/d, H_i/L
ANFIS4	5	W/L, H_i/d, H_i/L
ANFIS5	Total	S/D, W/L, H_i/d, H_i/L
ANFIS6	Total	S/D, W/L, H_i/d

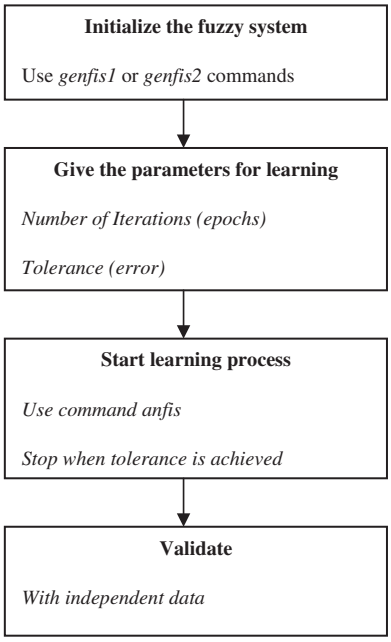

Fig. 4. ANFIS procedure.

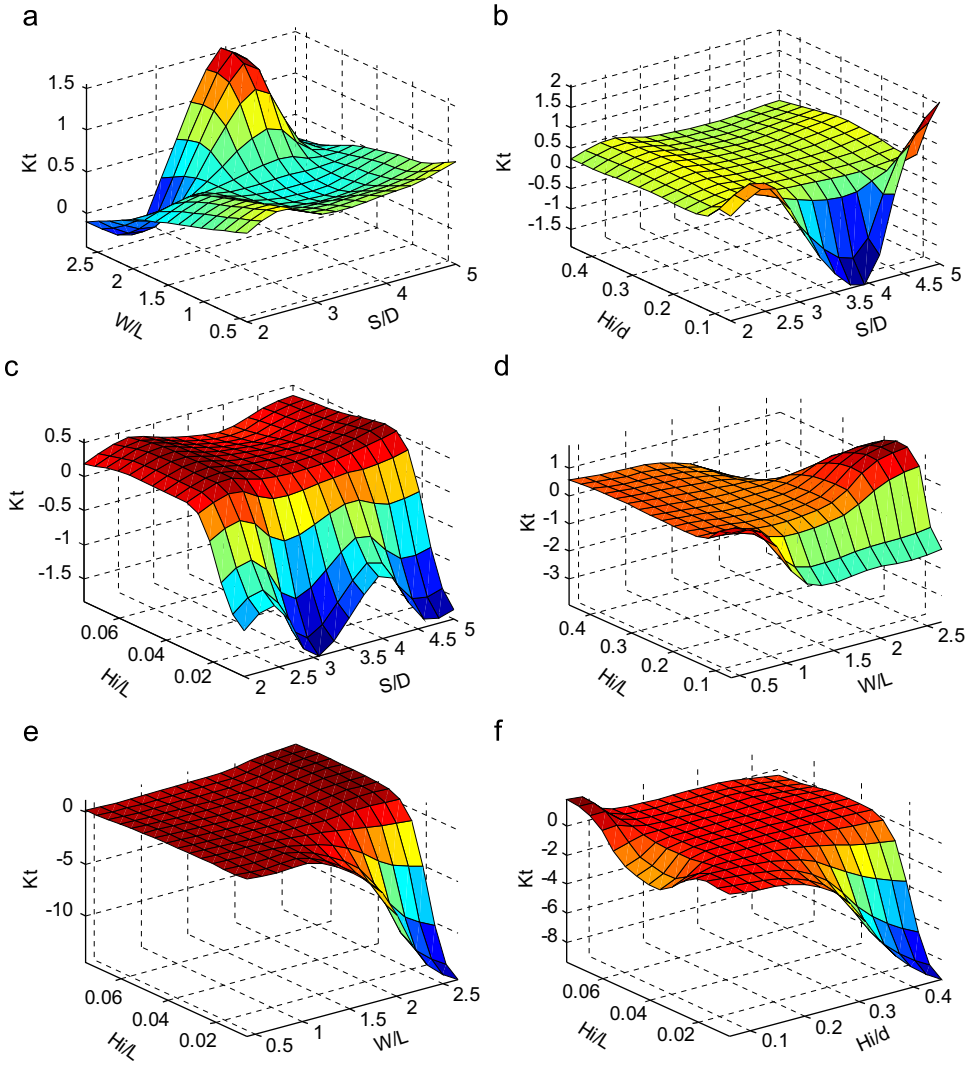

Fig. 3. Variation of measured K_t: (a) S/D & W/L, (b) S/D & Hi/d, (c) S/D & Hi/L, (d) W/L & Hi/d, (e) W/L & Hi/L and (f) Hi/d & Hi/L.

of membership functions is determined by trial and error. In the second step, parameters for learning are set with the number of iterations and tolerance. Once the learning parameters are set, an *anfis* command is used for learning, an *anfis* uses a hybrid learning algorithm to identify parameters of sugeno-type fuzzy inference systems.

An ANFIS distinguishes itself from normal fuzzy logic systems by the adaptive parameters, i.e. both the premise and consequent parameters are adjustable. The most remarkable feature of the ANFIS is its hybrid learning algorithm. The adaptation process of the parameters of the ANFIS is divided into two steps. For the first step of consequent parameters training, Least Squares method (LS) is used because the output of an ANFIS is a linear combination of the consequent parameters. The premise parameters are fixed at this step. After the consequent parameters have been adjusted, the approximation error is back-propagated through every layer to update the premise parameters as the second step. This part of the adaptation procedure is based on the gradient descent principle, which is the same as in the training of the back-propagation neural network. The consequent parameters identified by the LS method are optimal in the sense of least squares under the condition that the premise parameters are fixed. Therefore, this hybrid learning algorithm is more effective than the pure gradient decent approach, as it reduces the search space dimensions of the original back propagation method. The pure back propagation learning process could easily be trapped into the local minima. When compared

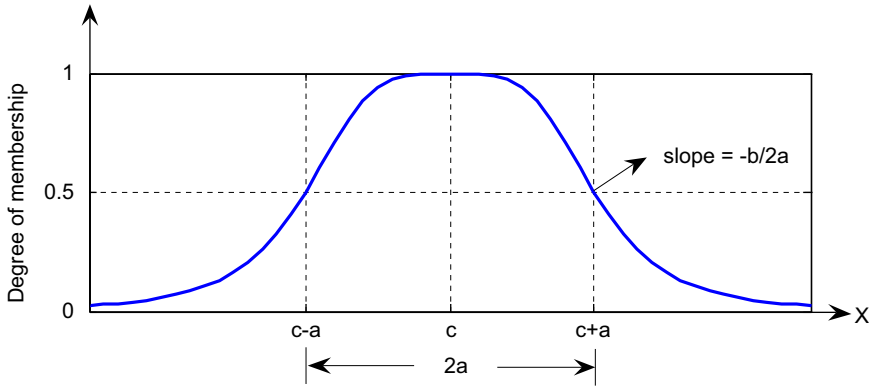

Fig. 5. Physical meaning of the parameters in the bell membership function.

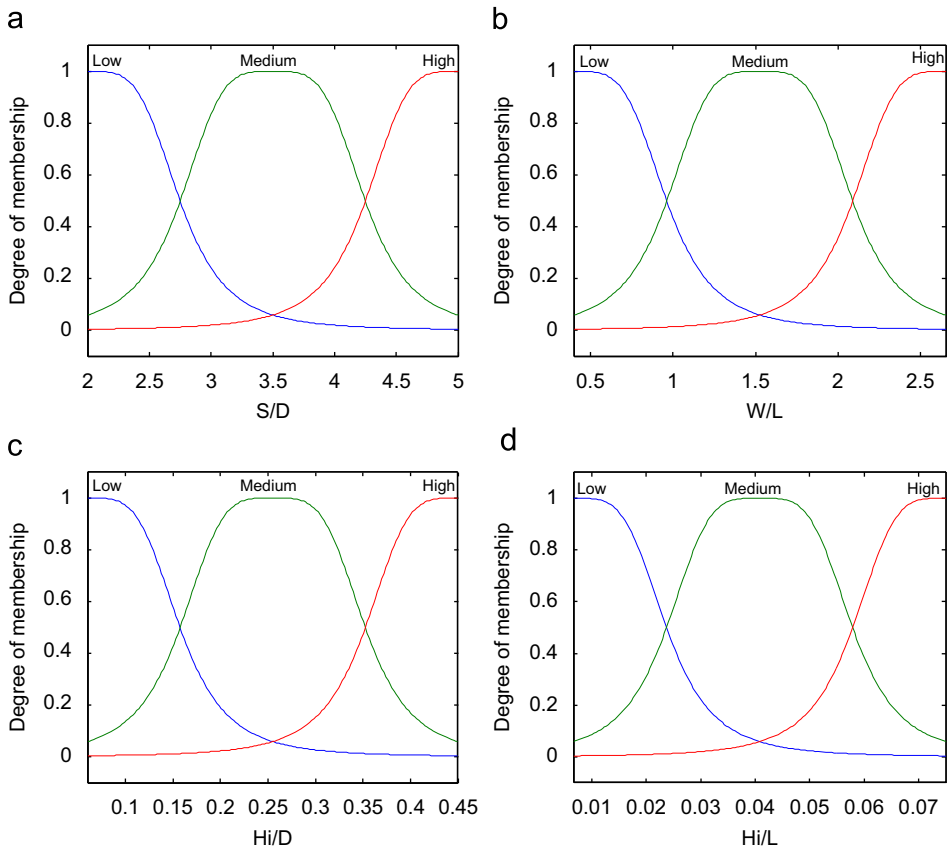

Fig. 6. Initial membership functions of input parameters (*X*-axis) for an ANFIS5 model: (a) S/D, (b) W/L, (c) Hi/d and (d) Hi/L.

with employing either one of the above two methods individually, the ANFIS converges with a smaller number of iteration steps with this hybrid learning algorithm. Once the tolerance is achieved, the learning process is stopped and validation is carried out by testing data set to compare the efficiency of the ANFIS model with an actual system.

In the present paper, three generalized bell membership functions have been assigned to each input variables as the initial membership function and is obtained by

$$\mu_{A_i}(X) = \frac{1}{1+[((X-c_i)/a_i)^2]^{b_i}} \tag{6}$$

where $\{a_i, b_i, c_i\}$ is the premise parameters set that changes the shape of the membership function with maximum equal to 1 and minimum equal to 0 and X is the input variable. The physical meaning of the parameters in bell membership function is given in Fig. 5, where a=half width of the bell function, b=slope at the crossover point (where degree of membership=0.5) and c=center of corresponding membership function. Each input variable is classified into three fuzzy categories with linguistic attributes as Low_i, Medium_i and High_i (i=1–3 for ANFIS1, ANFIS2, ANFIS3 and ANFIS4 models, whereas for an ANFIS5 model, i=1–4). Initial values of premise parameters before learning are set in such a way that the centers of the membership functions are equally spaced along the range of each input variable. Fig. 6 shows the initial membership function before learning for an ANFIS5 model associated with 4 inputs S/D, W/L, H_i/d and H_i/L. As the training process takes place values of a, b and c change, the bell shaped function vary accordingly, thus exhibiting various forms of membership functions on linguistic attributes A_i. Fig. 7 shows the final membership function after training for an ANFIS5 model. Table 4 lists the linguistic attributes A_i and the corresponding premise parameters for an ANFIS5 model. The hybrid learning algorithm that combines least square method with gradient descent method is used to adjust the parameters of the membership function.

Fig. 8 shows the fuzzy rule architecture for an ANFIS5 model with generalized bell membership function. The architecture shown in Fig. 8 consists of 81 fuzzy rules and 3 generalized bell membership function associated with 4 inputs S/D, W/L, H_i/d and H_i/L, whereas ANFIS1, ANFIS2, ANFIS3 and ANFIS4 model consists of 27 rules and 3 generalized bell membership function associated with three inputs W/L, H_i/d and H_i/L.

In ANFIS models, product inference rules are used at the fuzzification level and weighted average is used as defuzzifier.

The fuzzy $IF-THEN$rules for an ANFIS4 model after training are shown in Table 5.

Rule 1. If W/L is Low and H_i/d is Low and H_i/L is Low then,

$$K_t = \vec{c}_1.\vec{X} \tag{7}$$

Table 4
Premise parameters for an ANFIS5 model.

A	a_i	b_i	c_i
Low_1	0.7534	1.9998	2.0027
Medium_1	0.7492	2.0001	3.5021
High_1	0.7465	2.0003	5.0025
Low_2	0.5635	1.9998	0.3999
Medium_2	0.5655	1.9998	1.5219
High_2	0.5680	1.9997	2.6477
Low_3	0.0311	2.0016	0.0645
Medium_3	0.1087	2.0017	0.2110
High_3	0.1425	1.9989	0.4232
Low_4	0.0122	0.0007	0.0000
Medium_4	0.0118	1.9994	0.0449
High_4	0.0405	1.9992	0.0874

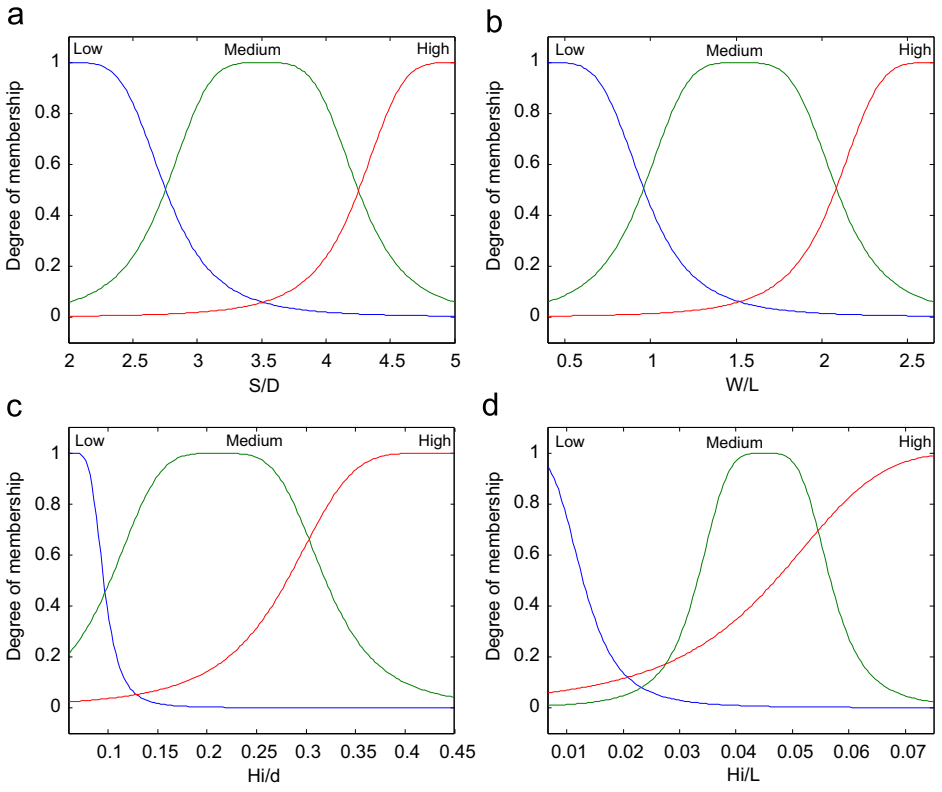

Fig. 7. Final membership functions of input parameters (X-axis) for an ANFIS5 model: (a) S/D, (b) W/L, (c) Hi/d and (d) Hi/L..

where $\vec{X}=[W/L,\ H_i/d,\ H_i/L,\ 1]$ and $\vec{c}_i$ is the ith row of the consequent parameter matrix C, as shown below.

$$C=\begin{bmatrix}
-0.2681 & -9.6906 & 29.4654 & 1.9173\\
-0.0301 & 30.4673 & -66.7380 & -1.1623\\
6.9865 & -4.5467 & 0.7491 & 0.6122\\
0.3117 & 0.8894 & -0.0868 & 1.1323\\
-0.7276 & 2.0967 & -14.4043 & 1.2034\\
0.8873 & -2.5686 & 29.4500 & -1.3169\\
-2.8564 & 47.1644 & -12.1817 & -12.9159\\
-0.0590 & -4.8697 & 24.0908 & 1.4401\\
-0.5679 & 2.2597 & 2.4840 & -0.0311\\
-0.6248 & 2.6189 & 26.7273 & 1.5391\\
0.6096 & -2.5181 & 9.3327 & -0.9857\\
4.0613 & -17.5433 & -0.4962 & 8.6854\\
-0.0706 & -15.0819 & 82.7353 & 2.0097\\
-0.2997 & 4.0968 & -20.6645 & 0.7287\\
0.0506 & -0.1335 & 12.2483 & -0.5003\\
-7.2845 & 10.6947 & 24.3701 & 5.7094\\
0.3424 & -2.0854 & 17.9905 & 0.0653\\
-0.1456 & 0.8293 & -2.4469 & 0.4715\\
-0.3445 & -18.8356 & -16.1056 & 3.1411\\
-0.0299 & 14.9003 & -12.4531 & -1.1065\\
6.8129 & 1.2283 & 0.0817 & 4.6369\\
-2.1517 & -1.2561 & 2.1870 & 4.0987\\
-0.5506 & 6.3736 & -2.4610 & 0.7510\\
0.0532 & 6.4288 & -4.1597 & -1.3002\\
7.1512 & -0.9702 & 0.1986 & -5.5973\\
-0.9720 & 2.0068 & 2.6307 & -0.4460\\
-0.1326 & 3.6693 & -6.2225 & -0.1971
\end{bmatrix}$$

5. Results and discussion

To study effectiveness of the approach, statistical comparison of measured and predicted values of K_t, correlation coefficient (CC) is used, which is defined as

$$CC=\frac{\sum_{i=1}^{N}(K_{tmi}-\overline{K_{tm}})(K_{tpi}-\overline{K_{tp}})}{\sqrt{\sum_{i=1}^{N}(K_{tmi}-\overline{K_{tm}})^2}\sqrt{\sum_{i=1}^{N}(K_{tpi}-\overline{K_{tp}})^2}} \tag{8}$$

where K_{tmi} and K_{tpi} represents the measured and predicted wave transmission coefficient, respectively, $\overline{K_{tm}}$ and $\overline{K_{tp}}$ are the mean value of measured and predicted observations, N is the number of observations. Higher the CC value better is the agreement between the measured and predicted values of K_t. Apart from this, other statistical measures computed are root-mean-square error (*RMSE*), and scatter index (*SI*). These are defined as

$$RMSE=\sqrt{\frac{1}{N}\sum_{i-1}^{N}\left(K_{tmi}-K_{tpi}\right)^2} \tag{9}$$

$$SI=\frac{RMSE}{\overline{K_{tm}}} \tag{10}$$

Statistical measures computed using trained and test data are shown in Table 6, trained and test data are used to compare the models results, all the ANFIS models have shown CCs higher than 0.9600 for trained data, whereas in case of test data it is more than 0.9500. *RMSE* is less than or equal to 0.044187 for training data and 0.051074 for test data, whereas the *SI* is less than or equal to 0.087728 for trained data and 0.102296 for test data. The trained and test results (CCs) of all ANFIS models are shown in Table 6 and Figs. 9–13. Experimental data show that K_t is better with an increase in *S/D* values, but it is noticed that the CCs between measured and predicted K_t increase with an *S/D* for ANFIS1, ANFIS2 and ANFIS3 models, whereas it is not true in case of an ANFIS4 model. Even though there is an improved relation with an increase of an *S/D* as seen from ANFIS1, ANFIS2 and ANFIS3 (Table 6). An ANFIS4 shows marginally lower values of CCs. This also indicates that an ANFIS3 model shows optimal K_t prediction in the present study. The highest correlation coefficient (CC Train=0.9786, CC Test=0.9698) is obtained for an ANFIS3 model. Increase or decrease in an *S/D* ratio does not show a clear relation in an

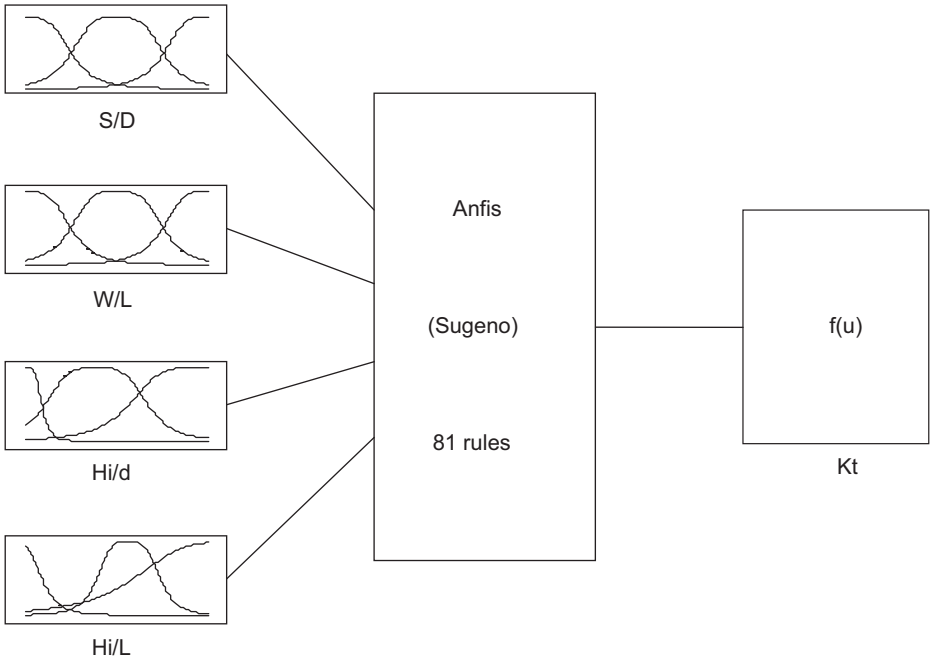

Fig. 8. Fuzzy rule architecture of the generalized bell membership function for an ANFIS5 model.

Table 5
Fuzzy *IF–THEN* rules after training for an ANFIS4 model.

Rule	W/L	H_i/d	H_i/L	K_t
1	Low	Low	Low	$\vec{c}_1 \cdot \vec{X}$
2	Low	Low	Medium	$\vec{c}_2 \cdot \vec{X}$
3	Low	Low	High	$\vec{c}_3 \cdot \vec{X}$
4	Low	Medium	Low	$\vec{c}_4 \cdot \vec{X}$
5	Low	Medium	Medium	$\vec{c}_5 \cdot \vec{X}$
6	Low	Medium	High	$\vec{c}_6 \cdot \vec{X}$
7	Low	High	Low	$\vec{c}_7 \cdot \vec{X}$
8	Low	High	Medium	$\vec{c}_8 \cdot \vec{X}$
9	Low	High	High	$\vec{c}_9 \cdot \vec{X}$
10	Medium	Low	Low	$\vec{c}_{10} \cdot \vec{X}$
11	Medium	Low	Medium	$\vec{c}_{11} \cdot \vec{X}$
12	Medium	Low	High	$\vec{c}_{12} \cdot \vec{X}$
13	Medium	Medium	Low	$\vec{c}_{13} \cdot \vec{X}$
14	Medium	Medium	Medium	$\vec{c}_{14} \cdot \vec{X}$
15	Medium	Medium	High	$\vec{c}_{15} \cdot \vec{X}$
16	Medium	High	Low	$\vec{c}_{16} \cdot \vec{X}$
17	Medium	High	Medium	$\vec{c}_{17} \cdot \vec{X}$
18	Medium	High	High	$\vec{c}_{18} \cdot \vec{X}$
19	High	Low	Low	$\vec{c}_{19} \cdot \vec{X}$
20	High	Low	Medium	$\vec{c}_{20} \cdot \vec{X}$
21	High	Low	High	$\vec{c}_{21} \cdot \vec{X}$
22	High	Medium	Low	$\vec{c}_{22} \cdot \vec{X}$
23	High	Medium	Medium	$\vec{c}_{23} \cdot \vec{X}$
24	High	Medium	High	$\vec{c}_{24} \cdot \vec{X}$
25	High	High	Low	$\vec{c}_{25} \cdot \vec{X}$
26	High	High	Medium	$\vec{c}_{26} \cdot \vec{X}$
27	High	High	High	$\vec{c}_{27} \cdot \vec{X}$

Table 6
ANFIS models with statistical measures for train and test data.

Model	CC Train	CC Test	Train data		Test data	
			RMSE	*SI*	*RMSE*	*SI*
ANFIS1	0.9649	0.9510	0.044187	0.087728	0.051074	0.102296
ANFIS2	0.9706	0.9528	0.031676	0.059149	0.038682	0.072278
ANFIS3	0.9786	0.9698	0.026438	0.044892	0.030780	0.053178
ANFIS4	0.9776	0.9674	0.032783	0.049827	0.039505	0.060767
ANFIS5	0.9723	0.9635	0.037269	0.065217	0.043068	0.076833
ANFIS6	0.9469	0.9378	0.05127	0.089716	0.055775	0.099503

increase or decrease of CCs, *RMSE* and *SI* estimated for train and test data. Taking this into view, it was decided to study over a range of an *S/D* on K_t. An input parameter, an *S/D* is added to form an ANFIS5 model (Table 3).

In order to assess the influence of input parameters, principal component analysis (PCA) is carried out. PCA is simple, non-parametric method for extracting relevant information from confusing data sets (Shlens, 2009). It transfers the data set onto different axes orthogonal to each other in the data space. The projections of the data on those vectors are the principal components and are found by calculating the eigenvectors of the data correlation matrix. The corresponding eigen values give an indication of the amount of information that the respective principal components represent. Thus by discarding those components, which explains a negligible part of the data variance, a high rate of data compression can be obtained.

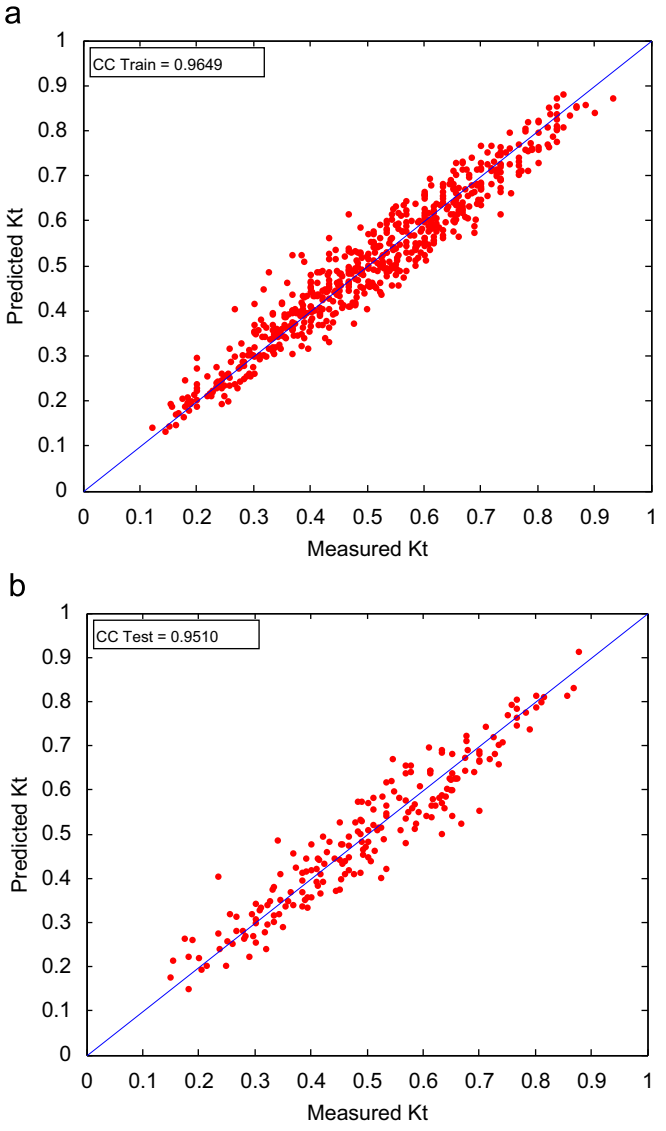

Fig. 9. Comparison of predicted and measured K_t for an ANFIS1 model: (a) Trained Data and (b) Test Data.

PCA estimates eigen values and variances of four non-dimensional parameters for each component, as shown in Table 7. The first component alone accounts for 84.914% of the total variance, the second component alone accounts for 14.431% and the 3rd and 4th components together account less than 1%, respectively. According to PCA, the first two components together account more than 99%. The factorial weights of the four components are shown in Table 8. This shows the first principal component has strong relation to the *S/D*, and the second principal component has strong relation to *W/L*. In fact, first principal component reflect the porosity parameter accounts for 84.914% of the total variance and the second principal component reflects the relative breakwater width, which accounts for 14.431%. From this study it is observed that H_i/L is the least influential parameter.

Based on the PCA study considering the first three input parameters, an ANFIS6 model shows CC of K_t, for Train=0.9469 and for Test=0.9378 (Table 6 and Fig. 14).

After conducting computer simulation on trained and test data of an ANFIS5 model, CCs are calculated between measured and predicted K_t are shown in Table 6 and Fig. 13. An ANFIS5 model predictions are very realistic when compared with the measured

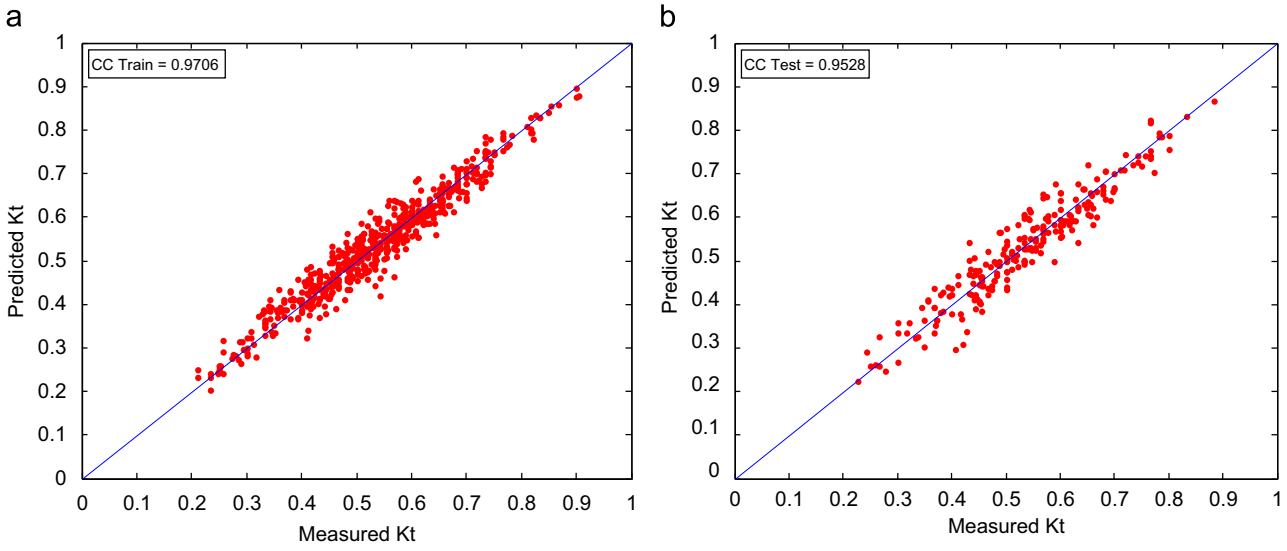

Fig. 10. Comparison of predicted and measured K_t for an ANFIS2 model: (a) Trained Data and (b) Test Data.

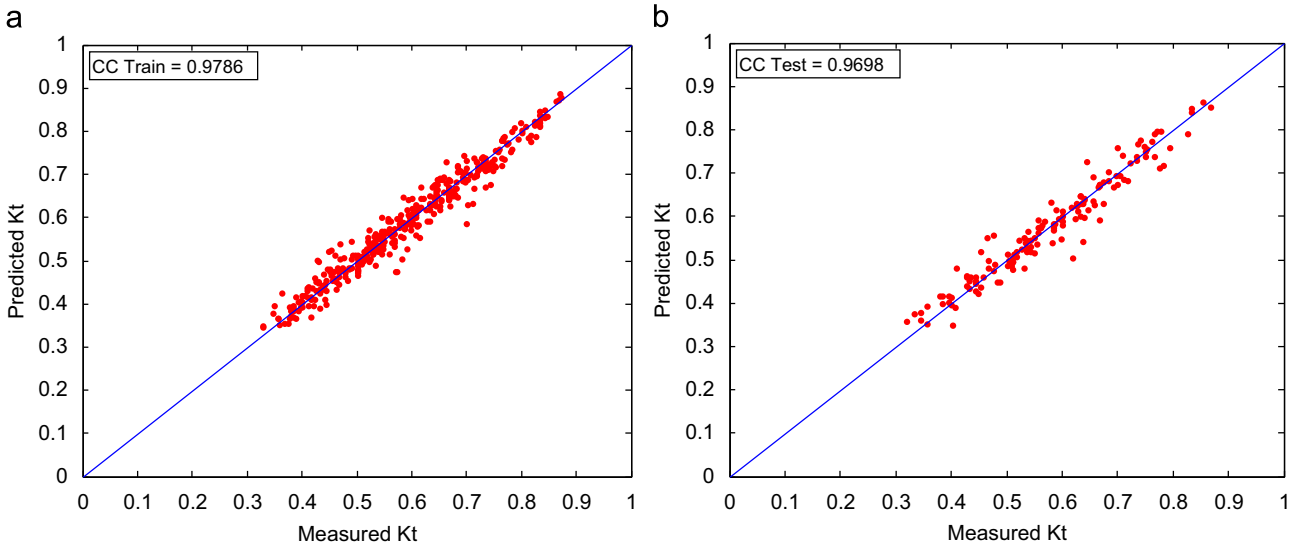

Fig. 11. Comparison of predicted and measured K_t for an ANFIS3 model: (a) Trained Data and (b) Test Data.

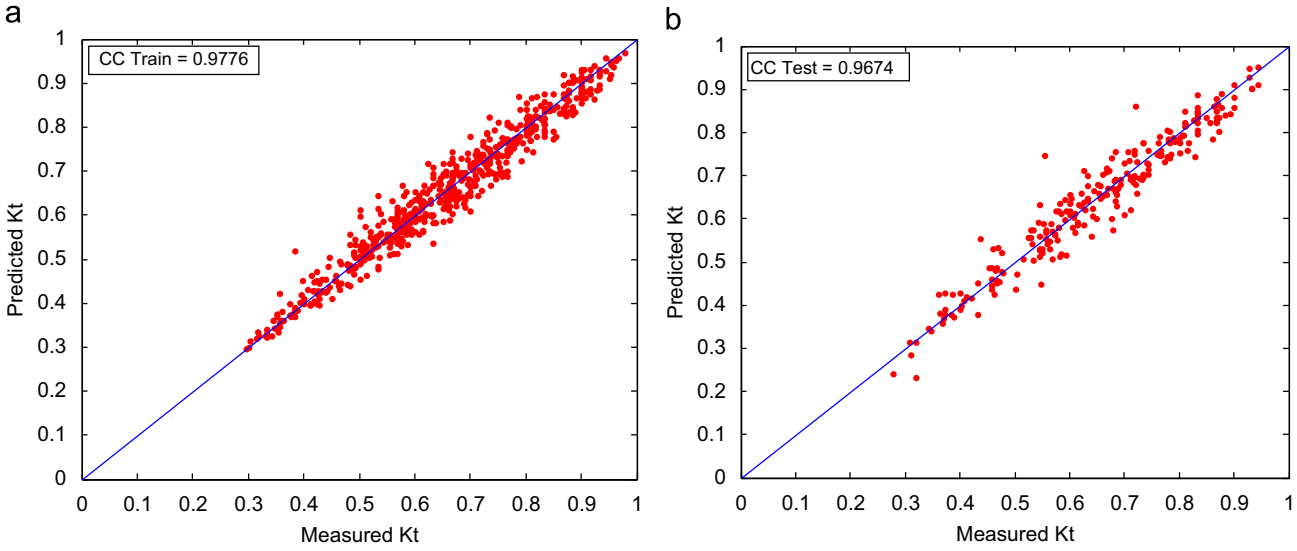

Fig. 12. Comparison of predicted and measured K_t for an ANFIS4 model: (a) Trained Data and (b) Test Data.

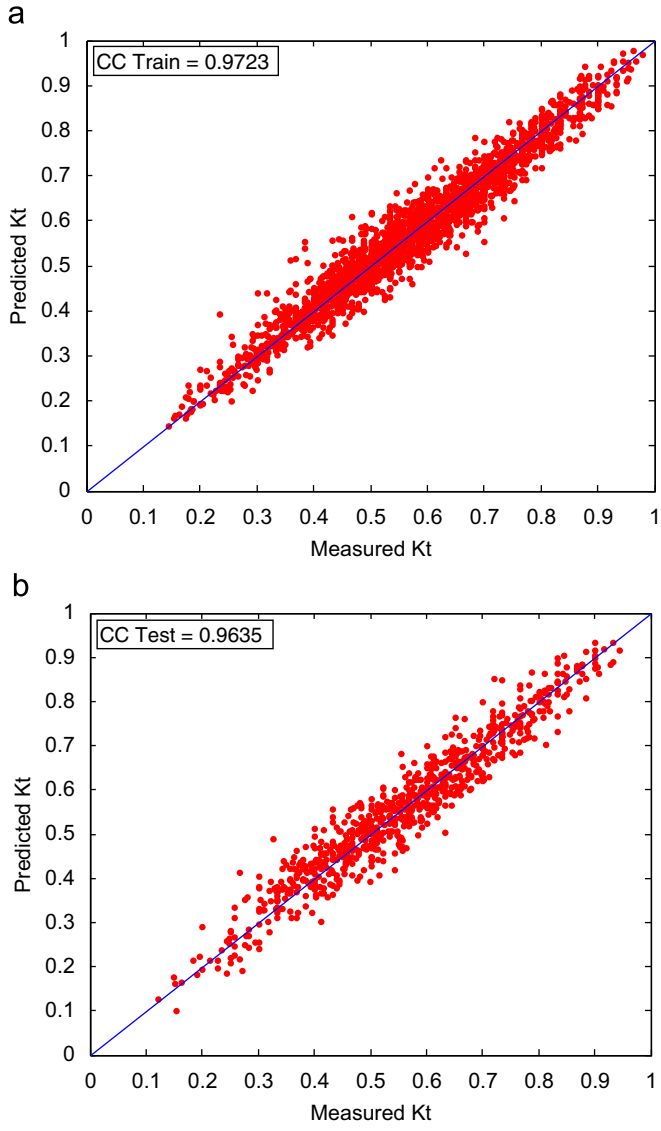

Fig. 13. Comparison of predicted and measured K_t for an ANFIS5 model: (a) Trained Data and (b) Test Data.

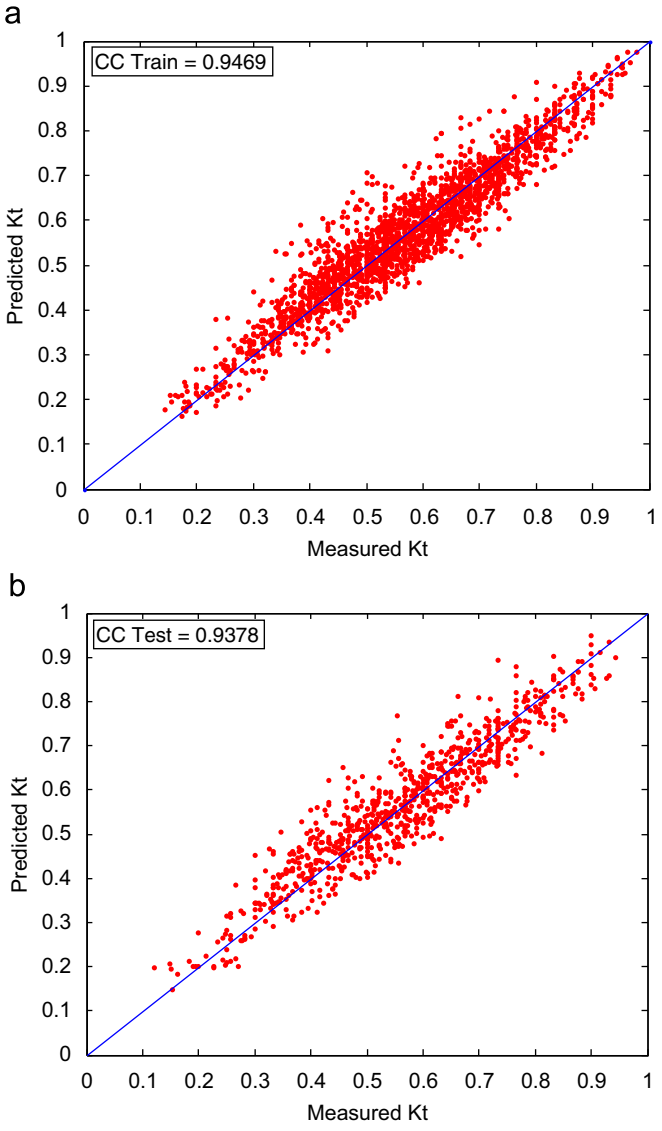

Fig. 14. Comparison of predicted and measured K_t for an ANFIS6 model: (a) Trained Data and (b) Test Data.

Table 7
Principal component analysis.

Principal components numbers	PC1	PC2	PC3	PC4
Eigen value	1.35350	0.23002	0.01038	0.00005
% Variance	84.914	14.431	0.652	0.003
Cumulative % variance	84.914	99.345	99.997	100.000

Table 8
Factor loading of principal components.

Input parameters	PC1	PC2	PC3	PC4
S/D	**−0.99991**	0.01327	0.00107	0.00025
W/L	0.01328	**0.99966**	−0.02056	−0.00944
H_i/d	0.00074	−0.02164	−0.99089	−0.13293
H_i/L	0.00048	0.00661	−0.13310	0.99108

values (CC Train = 0.9723, CC Test = 0.9635), whereas the *RMSE* and *SI* are 0.037269 and 0.065217 for train data, and 0.043068 and 0.076833 for test data, respectively. An ANFIS5 model performed better than ANFIS1 and ANFIS2 models, whereas the performance is almost same when compared with ANFIS3 and ANFIS4 models. Performance of an ANFIS model depends upon the input parameters chosen to train the model. Considering an S/D as an input parameter, there is a better CC between measured and predicted K_t when compared with ANFIS1 and ANFIS2. This clearly proves that an S/D plays an important role to train ANFIS5 model to map an input–output relation.

From ANFIS5 and ANFIS6, CCs of K_t show very little variation as H_i/L is the least influential parameter.

The same data set had been used for estimating K_t using an ANN (Mandal et al., 2009). CCs of K_t are shown in Table 9. From Tables 6

Table 9
ANN models with correlation coefficients of K_t.

Model	S/D Ratio	CC Train	CC Test
ANN1	2	0.9552	0.9504
ANN2	3	0.9506	0.9404
ANN3	4	0.9642	0.9601
ANN4	5	0.9672	0.9649
ANN5	Total	0.9537	0.9488

and 9, it is observed that the ANFIS models yield higher CCs as compared to that of ANN models.

6. Conclusions

Prediction of the wave transmission coefficient is necessary in order to design a floating breakwater. Researchers have carried out tremendous work dealing with floating breakwater, but they failed to give a simple mathematical model for these structures to predict the wave transmission. Number of studies has been carried out considering a floating breakwater with a simple form by introducing certain simplifying assumptions, which shows less improvement. In this paper, ANFIS models are developed to predict the wave transmission of HIMMFPB. The input parameters that influence the K_t of HIMMFPB such as S/D, W/L, H_i/d and H_i/L are considered. Based on these input parameters, six ANFIS models are constructed to predict the transmission coefficient of HIMMFPB. In ANFIS1, ANFIS2, ANFIS3 and ANFIS4 structures first order Sugeno model containing 27 rules and 3 generalized bell membership functions are used, whereas for ANFIS5 structure first order Sugeno model containing 81 rules and 3 generalized bell membership functions are used. All ANFIS models use product inference rule at the fuzzification level and the weighted average is used as defuzzifier. Hybrid learning algorithm that combines least square method with gradient descent method is used to adjust the parameters of the membership function.

Computer simulation on train and test data of all ANFIS models shows the effectiveness of the approach in terms of statistical measures, such as correlation coefficient, root mean square error and scatter index.

Based on the PCA, it is observed that S/D and W/L are the most significant parameters. Whereas H_i/L is the least influencing parameter and variation of correlations (ANFIS5 and ANFIS6 models) is negligible. It is also concluded that S/D and W/L play an important role as inputs for training ANFIS models.

ANFIS models outperformed ANN models for predicting K_t.

Trained ANFIS can be utilized to provide a fast and reliable solution in prediction of the wave transmission for HIMMFPB, thereby making ANFIS as an alternate approach to map the wave-structure interactions of HIMMFPB.

Acknowledgements

The authors are grateful to the Director, and Head, Department of Applied Mechanics and Hydraulics, NITK, Surathkal, India, for support and encouragement provided to them and for permission to publish the paper. Thanks are also due to Ministry of Earth Sciences, GOI for sponsoring the project on HIMMFPB at NITK, Surathkal, India.

References

Bakhtyar, R., Ghaheri, A., Yeganeh-Bakhtiary, A., Baldock, T.E., 2008b. Longshore sediment transport estimation using a fuzzy inference system. Applied Ocean Research 30, 273–286.

Bakhtyar, R., Yeganeh-Bakhtiary, A., Ghaheri, A., 2008a. Application of neuro-fuzzy approach in prediction of runup in swash zone. Applied Ocean Research 30, 17–27.

Bateni, S.M., Jeng, D.S., 2007. Estimation of pile group scour using adaptive neuro-fuzzy approach. Ocean Engineering 34, 1344–1354.

Bishop, T.C., 1982. Floating tire breakwater design comparison. Journal of Waterway, Port, Coastal and Ocean Engineering, ASCE 108 (3), 421–426.

Chang, H.K., Lin, L.C., 2006. Multi-point tidal prediction using artificial neural network with tide-generating forces. Coastal Engineering 53, 857–864.

Deepak, J.C., 2006. Laboratory investigations on horizontal interlaced multi-layer moored floating pipe breakwater. M.Tech Thesis, Department of Applied Mechanics and Hydraulics, N.I.T.K., Surathkal, Karnataka, India, July, 1–113.

Deo, M.C., Jagdale, S.S., 2003. Prediction of breaking waves with neural networks. Ocean Engineering 30, 1163–1178.

Deo, M.C., Jha, A., Chaphekar, A.S., Ravikant, K., 2001. Neural networks for wave forecasting. Ocean Engineering 28, 889–898.

Gunaydin, K., 2008. The estimation of monthly mean significant wave heights by using artificial neural network and regression methods. Ocean Engineering 35, 1406–1415.

Harms, V.W., 1979. Design criteria for floating tire breakwater. Journal of Waterway, Port, Coastal and Ocean Engineering, ASCE 106 (2), 149–170.

Harris, A.J., Webber, N.B., 1968. A floating breakwater. In: Proceedings of the 11th Coastal Engineering Conference, London, England, 1049–1054.

Hegde, A.V., Kamath, K., Magadum, A.S., 2007. Performance characteristics of horizontal interlaced multilayer moored floating pipe breakwater. Journal of Waterway, Port, Coastal and Ocean Engineering, ASCE 133 (4), 275–285.

Homma, M., Horikawa, K., Mochizuki, H., 1964. An experimental study of floating breakwaters. In: Proceedings of the 10th Coastal Engineering Conference, Japan, vol. 7, 85–94.

Chang, H-K., Chien, W-A., 2006. A fuzzy-neural hybrid system of simulating typhoon waves. Coastal Engineering 53, 737–748.

Jagadisha, Y.S., 2007. Laboratory investigations on horizontal interlaced multi-layer moored floating pipe breakwater model. M.Tech Thesis, Department of Applied Mechanics and Hydraulics, NITK Surathkal, Karnataka.

Jang, J.S.R., 1993. ANFIS: adaptive-networked-based fuzzy inference systems. IEEE Transactions on Systems, Man, and Cybernetics 23 (3), 665–685.

Jang, J.S.R., Sun, C.T., Mizutani, E., 1997. Neuro-fuzzy and soft computing, PTR. Prentice Hall.

Jeng, D.S., Cha, D., Blumenstein, M., 2004. Neural network for the prediction of wave induced liquefaction potential. Ocean Engineering 31, 2073–2086.

Kamat, K., 2010. Hydrodynamics performance characteristics of horizontal interlaced multi-layer moored floating pipe breakwater—a physical model study. Ph.D. Thesis, Department of Applied Mechanics and Hydraulics, NITK Surathkal, Karnataka, India.

Kazeminezhad, M.H., Etemad-shahidi, A., Mousvi, S.J., 2005. Application of fuzzy inference system in the prediction of wave parameters. Ocean Engineering 32, 1709–1725.

Kennedy, R.J., Marsalek, J., 1968. Flexible porous floating breakwater. In: Proceedings of the 11th Coastal Engineering Conference, London, England, 1095–1103.

Leach, A.P., McDougal, G.W., Solitt, K.C., 1985. Hinged floating breakwater. Journal of Waterway, Port, Coastal and Ocean Engineering, ASCE 111 (5), 895–920.

Lee, T.L., Tsai, C.P., Lin, H.M., Fang, C.J., 2009. A combined thermo graphic analysis—neural network methodology for eroded caves in a sea wall. Ocean Engineering 36, 1251–1257.

Londhe, S.N., Deo, M.C., 2003. Wave tranquility studies using neural networks. Marine Structures 16, 419–436.

Mandal, S., Patil, S.G., Hegde, A.V., 2009. Wave transmission prediction of multilayer floating breakwater using neural network. In: Proceedings of the International Conference in Ocean Engineering, IIT Madras, Chennai, India, 574–585.

Mandal, S., Rao, S., Manjunatha, Y.R., 2007. Stability analysis of rubble mound breakwater using ANN. In: Proceedings of the Indian National Conference on Harbour and Ocean Engineering, INCHOE, NITK, Surathkal, 551–560.

Mani, J.S., 1991. Design of Y—frame floating breakwater. Journal of Waterways, Port, Coastal and Ocean Engineering, ASCE 117 (2), 105–118.

McCartney, L.B., 1985. Floating breakwater design. Journal of Waterway, Port, Coastal and Ocean Engineering, ASCE 111 (2), 304–318.

Murali, K., Mani, J.S., 1997. Performance of cage floating breakwater. Journal of Waterway, Port, Coastal and Ocean Engineering, ASCE 123 (4), 172–179.

Ozger, M., Zekai, S., 2006. Prediction of wave parameters by fuzzy logic approach. Ocean Engineering 34, 460–469.

Sannasiraj, S.A., Sundar, V., Sundaravadivelu, R., 1998. Mooring forces and motion response of pontoon-type floating breakwaters. Ocean Engineering 25 (1), 27–48.

Shlens, J., 2009. A tutorial on principal component analysis. Center for Neural Science, New York University New York City, NY 10003-6603 and Systems Neurobiology Laboratory Salk Institute for Biological Studies La Jolla, CA 92037.

Srinivasan, A., Nigam, M.J., 2008. Neuro-fuzzy based approach for inverse kinematics solution of industrial robot manipulators. International Journal of Computers, Communications and Control 3 (3), 224–234.

Sundar, V., Sundaravadivelu, R., Purushotham, S., 2003. Hydrodynamic characteristics of moored floating pipe breakwater in random waves. In: Proceedings of the Institution of Mechanical Engineers, Journal of Engineering Maritime Environment 217 (M), 95–108.

Sylaios, G., Bouchette, F., Tsihrintziz, V.A., Denamiel, C., 2009. A fuzzy inference system for wind wave modeling. Ocean Engineering 36, 1358–1365.

Takagi, T., Sugeno, M., 1985. Fuzzy identification of systems and its applications to modeling and control. IEEE Transactions on Systems, Man, and Cybernetics 15, 116–132.

Erdik, T., 2009. Fuzzy logic approach to conventional rubble mound structure design. Expert Systems with Applications 36, 4162–4170.

Tseng, C.M., Jan, C.D., Wang, J.S., Wang, C.M., 2007. Application of artificial neural networks in typhoon surge forecasting. Ocean Engineering 34, 1757–1768.

Wang, L.X., 1994. Adaptive Fuzzy Systems and Control, Design and Stability Analysis. PTR Prentice Hall.

Wang, L.X., 1997. A Course in Fuzzy Systems and Control. PTR Prentice Hall.

Yagci, O., Mercan, D.E., Cigizoglu, H.K., Kabdasli, M.S., 2005. Artificial intelligence methods in breakwater damage ratio estimation. Ocean Engineering 32, 2088–2106.

Zadeh, L.A., 1965. "Fuzzy sets". Information and Control 8, 338–353.